

# The effect of demographic stochasticity on predatory-prey oscillations

Solmaz Golmohammadi

*Department of Physics, Institute for Advanced Studies in  
Basic Sciences (IASBS), Zanjan, 45137-66731, Iran and  
The Abdus Salam International Centre for Theoretical Physics (ICTP),  
Strada Costiera 11, 34014 Trieste, Italy*

Mina Zarei\*

*Department of Physics, Institute for Advanced Studies  
in Basic Sciences (IASBS), Zanjan, 45137-66731, Iran*

Jacopo Grilli<sup>†</sup>

*Quantitative Life Sciences section, The Abdus Salam  
International Centre for Theoretical Physics (ICTP),  
Strada Costiera 11, 34014 Trieste, Italy*

## Abstract

The ecological dynamics of interacting predator and prey populations can display sustained oscillations, as for instance predicted by the Rosenzweig-MacArthur predator-prey model. The presence of demographic stochasticity, due to the finiteness of population sizes, alters the amplitude and frequency of these oscillations. Here we present a method for characterizing the effects of demographic stochasticity on the limit cycle attractor of the Rosenzweig-MacArthur. We show that an angular Brownian motion well describes the frequency oscillations. In the vicinity of the bifurcation point, we obtain an analytical approximation for the angular diffusion constant. This approximation accurately captures the effect of demographic stochasticity across parameter values.

## I. INTRODUCTION

The independent work of Alfred Lotka and Vito Volterra [1, 2] demonstrated over a century ago how predator-prey population dynamics can exhibit neutral oscillation, where the amplitude depends on the initial condition, with a fixed frequency. The critical assumption in the original formulation, ultimately giving rise to neutral oscillations, is that the growth rate of predators depends linearly on the density of preys (so-called linear functional responses). Their models were extended by Rosenzweig and MacArthur [3] to incorporate more realistic saturating functional responses (Holling type II [4]). In this setting, the dynamics converge to a stable limit cycle in certain parameter regimes. In that case, prey and predator populations oscillate with fixed frequency and amplitude, independently of initial conditions. Population oscillations have been observed in natural predator-prey ecosystems and confirmed by experiments [5–10], although there is ongoing debate regarding whether their origins are endogenous, as predicted by the Rosenzweig-MacArthur (RMA) model, or exogenous, arising for instance from periodic (e.g., seasonal) environmental fluctuations.

In reality, population dynamics are generally stochastic due to intrinsic or extrinsic factors. Extrinsic factors include environmental fluctuations such as weather, fires, and seasonality, as well as biotic disturbances. Earlier studies have examined the stochastic behavior of population dynamics and the impact of external noise on these dynamics [11–14]

---

\* mina.zarei@iasbs.ac.ir

† jgrilli@ictp.it

Intrinsic factors arise from demographic effects, where the discrete nature of populations leads to random and independent birth, death, and migration processes. Accurately capturing this inherent stochasticity is essential for understanding the complex dynamics and interactions that govern ecological systems. Various methods and formalisms have been developed to address this stochasticity, each with its own strengths and limitations tailored to specific research questions. These approaches can be explored both analytically and numerically, providing a comprehensive view of the dynamics within these intricate systems [15].

In our study, we present a novel analytical framework that models the noise affecting the phase of the limit cycle in a stochastic predator-prey system as angular Brownian motion. By approximating the limit cycle as an ellipse through the Van Kampen expansion of the master equation, we derive key insights into the system's behavior. Our findings are further validated through simulations using the Gillespie algorithm applied to a stochastic Rosenzweig-MacArthur model. This dual methodology, which integrates robust numerical simulations with analytical techniques, underscores the advantages of Individual-Based Models (IBMs) over traditional population-level and agent-based models, offering a deeper understanding of the effects of demographic stochasticity on predator-prey dynamics.

In section II, we introduce the stochastic Rosenzweig-MacArthur model. In Section III we present our results. First, we give an analytical approximation to find the mean frequency and the radius of the limit cycle close to the bifurcation point in the determining case. Second, we show that the perturbations along the limit cycle generated by demographic stochasticity can be approximated by an angular Brownian motion. Finally, we extract an analytic expression for the noise strength using Van Kampen system size expansion of the corresponding Fokker-Planck equation. Section IV presents discussion and concluding remarks.

## II. THE ROSENZWEIG-MACARTHUR PREDATOR-PREY MODEL

The Rosenzweig-MacArthur Predator-Prey (RMA) Model [3] provides a standard framework to study the coupled dynamics of predator and prey populations. The population

abundances of the prey ( $R$ ) and predators ( $F$ ) change in time accordingly to

$$\begin{aligned}\dot{R} &= aR - \frac{R^2}{2N} - \frac{sRF}{1 + s\tau R}, \\ \dot{F} &= -dF + \frac{sRF}{1 + s\tau R}.\end{aligned}\tag{1}$$

In the absence of predators ( $F = 0$ ), the preys grow logistically, with growth rate  $a$  and carrying capacity  $2Na$ . In the absence of prey ( $R = 0$ ) the predator population declines with the death rate  $d$ . The per-capita predation rate has a Holling type II functional response which saturates to  $1/\tau$  for large predator populations. The parameter  $\tau$  is the handling time of each prey. The base predation rate is equal to  $s$ .

Without loss of generality, we define  $d = 1$  (which corresponds to set the timescale of the system to be measured relatively to the predators lifespan) and set population abundances  $x = R/N$  and  $y = F/N$  to obtain

$$\begin{aligned}\dot{x} &= ax - \frac{x^2}{2} - \frac{\sigma xy}{1 + \sigma\tau x}, \\ \dot{y} &= -y + \frac{\sigma xy}{1 + \sigma\tau x},\end{aligned}\tag{2}$$

where  $\sigma = sN$ .

Equation 2 admits three distinct fixed points [3, 16, 17]

$$\begin{aligned}M_1 &= (x = 0, y = 0), \\ M_2 &= (x = 2a, y = 0), \\ M_3 &= \left( x = \frac{1}{\sigma(1 - \tau)}, y = \frac{2a\sigma(1 - \tau) - 1}{2\sigma^2(1 - \tau)^2} \right).\end{aligned}\tag{3}$$

The trivial fixed point  $M_1$  corresponds to the extinction of both species and is always unstable, as, in absence of predators, preys are always able to invade.  $M_2$  corresponds to the state that only the prey is present. This point is also unstable for where

$$\sigma > \sigma_0 = \frac{1}{2a(1 - \tau)}.\tag{4}$$

Under this condition, the predators are able to grow on a population of preys with density equal to its carrying capacity. The third fixed point  $M_3$  corresponds to coexistence between predators and preys and it is stable if

$$\sigma_0 < \sigma < \sigma^* = \frac{1 + \tau}{2a\tau(1 - \tau)}.\tag{5}$$

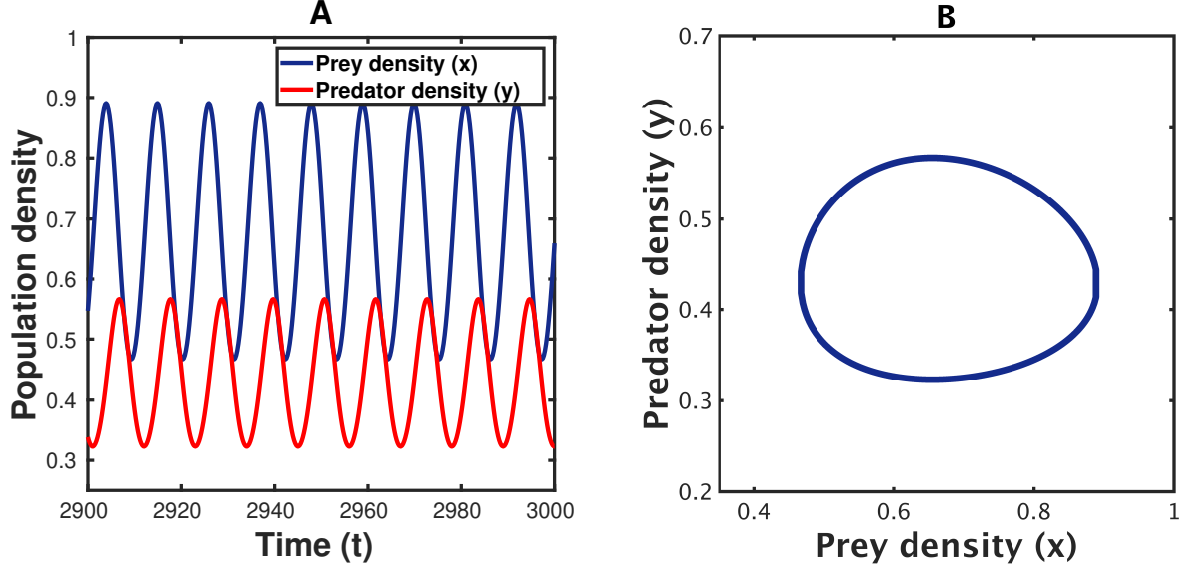


FIG. 1. Deterministic RMA model. (A) Oscillations of populations versus time, where blue and red correspond to prey and predator densities respectively. (B) The corresponding limit cycle in phase space. Parameters in these figures are  $\tau = 0.5$ ,  $a = 1$  and  $\sigma = 3.05$ .

For  $\sigma < \sigma_0$  the system converge to  $M_2$ . For  $\sigma > \sigma^*$ ,  $M_3$  is an unstable (as all the other fixed points) and the dynamics converges to a stable limit cycle as depicted in figure 1.

We generalize this deterministic model to include stochasticity by considering a discrete number of individuals  $F$  and  $R$ , which change with the following rates:

$$\begin{aligned}
 T(F, R + 1 | R, F) &= aR, \\
 T(F + 1, R - 1 | R, F) &= \frac{sRF}{1 + s\tau R}, \\
 T(F, R - 1 | R, F) &= \frac{R^2}{2N}, \\
 T(F - 1, R | R, F) &= F,
 \end{aligned} \tag{6}$$

where  $T(C_f | C_i)$  indicates the rate from initial configuration  $C_i$  to final configuration  $C_f$ .

These rates fully define the stochastic process that determines the dynamics of the system [17]. In the limit of  $N \rightarrow \infty$ , demographic stochasticity can be neglected and the trajectories can be approximated as the solutions of eq. 2.

Figure 2 displays one stochastic trajectory of the RMA system (generated using the Gillespie algorithm) in the parameter regime where a limit cycle in the deterministic system is expected. While the trajectories are noisy, they still resemble the deterministic limit cycle.

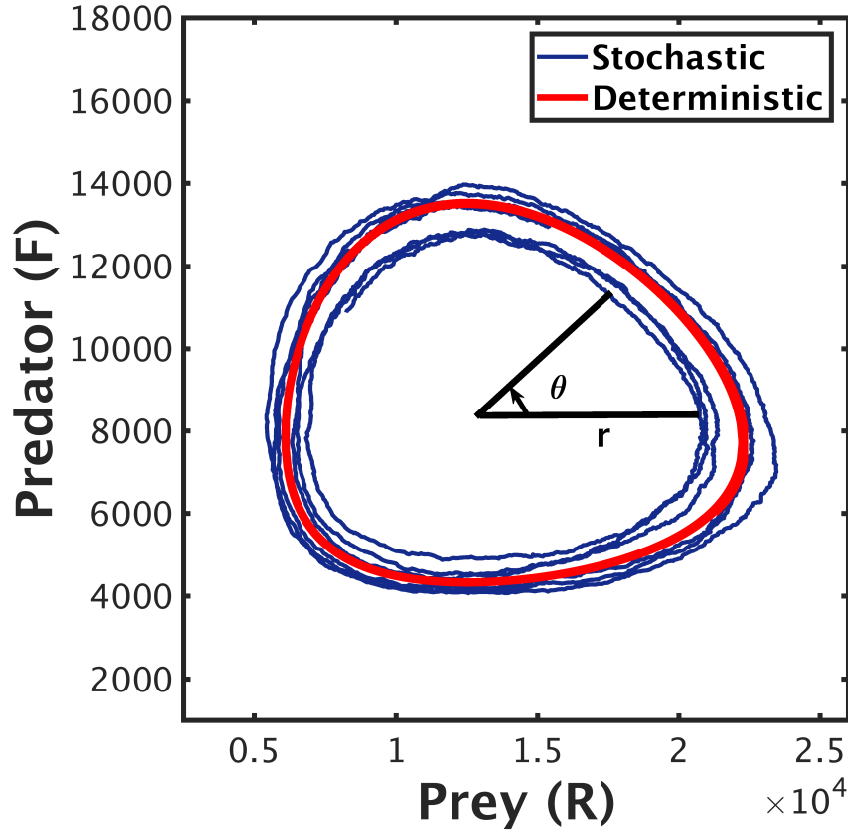


FIG. 2. Limit cycles of the deterministic and Stochastic RMA models. Radius ( $r$ ) and phase ( $\theta$ ) in the phase space has been determined in the figure. Deterministic limit cycle has been distinguished by red color. Parameters in these figures are  $\tau = 0.5$ ,  $a = 1$ ,  $N = 20000$  and  $\sigma = 3.2$ .

### III. RESULTS

In the previous section, we provided the definition of the deterministic and stochastic RMA model. In the parameter regime where a limit cycle occurs, the stochastic trajectory still displays an oscillatory behavior. In this section, we linearize the fluctuations around the deterministic attractor and quantify the effect of stochasticity. We then compare the analytical results to numerical simulations.

#### A. Elliptical Approximation of the Limit Cycle

In order to quantify the noise strength along the limit cycle, it is convenient to rewrite the differential equations in the polar phase space. We can approximate the shape of the

limit cycle to an ellipse, when the amplitude of the oscillations is small. In particular, this occurs when the parameter  $\sigma/\sigma^* \rightarrow 1^+$ , and in that case the oscillations occur in the vicinity of the  $M_3$ . It is convenient to introduce  $\gamma = \frac{\sigma - \sigma^*}{\sigma^*}$ . Our approximation holds for small and positive values of  $\gamma$ . We define  $dx$  and  $dy$  as follows:

$$\begin{aligned} dx &= r(t) \cos \theta(t), \\ dy &= r(t) \epsilon \sin \theta(t), \end{aligned} \tag{7}$$

where  $dx = (x - x_f)$ ,  $dy = (y - y_f)$  and  $M_3 = (x_f, y_f)$ . The variable  $\theta$  is the phase variable on the limit cycle centered at the mentioned fixed point ( $M_3$ ), which is calculated as follows:

$$\theta = \tan^{-1} \left( \frac{y - y_f}{x - x_f} \right). \tag{8}$$

The phase value goes from 0 to  $2\pi$  as the system evolves by time and completes a cycle in the phase-space, as illustrated in Figure 2. By expanding the equation 2 around  $(x_f, y_f)$  and using equation 7, one can find  $\dot{r}$  and  $\dot{\theta}$  (see details in the supplementary materials). Under this approximation, we obtained the following expressions for the mean frequency ( $\omega$ ) and the mean radius ( $\langle r \rangle$ )

$$\begin{aligned} \omega &= \epsilon = \sqrt{a(1 - \tau) - \frac{1}{2\sigma}}, \\ \langle r \rangle &= \frac{2a \sqrt{\frac{\gamma\tau(1 + \tau)}{1 + \gamma - \tau + \gamma\tau}}}{1 + \gamma + \tau + \gamma\tau}. \end{aligned} \tag{9}$$

We provide a confirmation of the analytical results using direct numerical simulation of the deterministic and of the stochastic RMA models. Figure 3 compares the time evolution of the phase and radius of the limit cycle. Note that, due to the fact that the limit-cycle does not have a perfect elliptic shape, we observe oscillations of both radius and frequency of oscillations. Nevertheless, our analytical approximation for mean radius is in agreement with the simulation results.

Figure 4 illustrates the dependency of the mean radius ( $\langle r \rangle$ ) versus system parameters  $\tau$  and  $\sigma$  obtained using stochastic simulation and analytical approximation. One can see that, as expected, our approximation matches the simulations when the limit cycle trajectory remains in the vicinity of the fixed point  $M_3$ , i.e. for small values of  $\gamma$ . As the amplitude of the limit cycle increases (i.e., when we increase the value of  $\gamma$ ) the approximation become

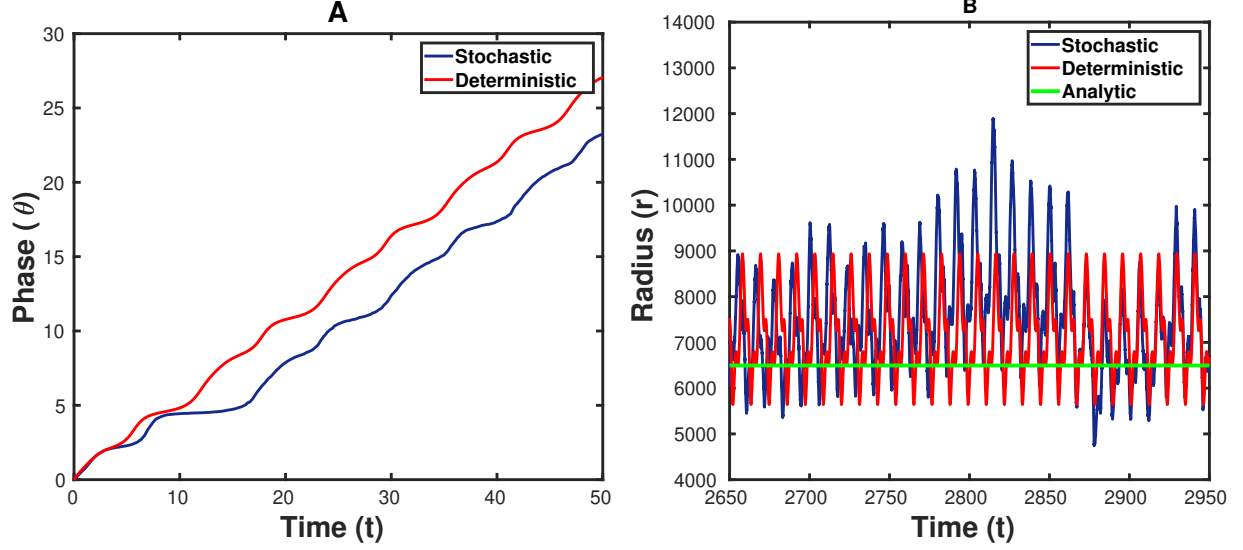


FIG. 3. Comparison of deterministic, stochastic and analytic approximation of RMA model. (A) Phase versus time ( $N = 1800$ ). (B) Radius versus time ( $N = 20000$ ). Parameters in these figures are  $\tau = 0.5$ ,  $a = 1$  and  $\sigma = 3.2$ .

less and less accurate. This mismatch occurs because the shape of the limit cycle becomes more and more different from an ellipse.

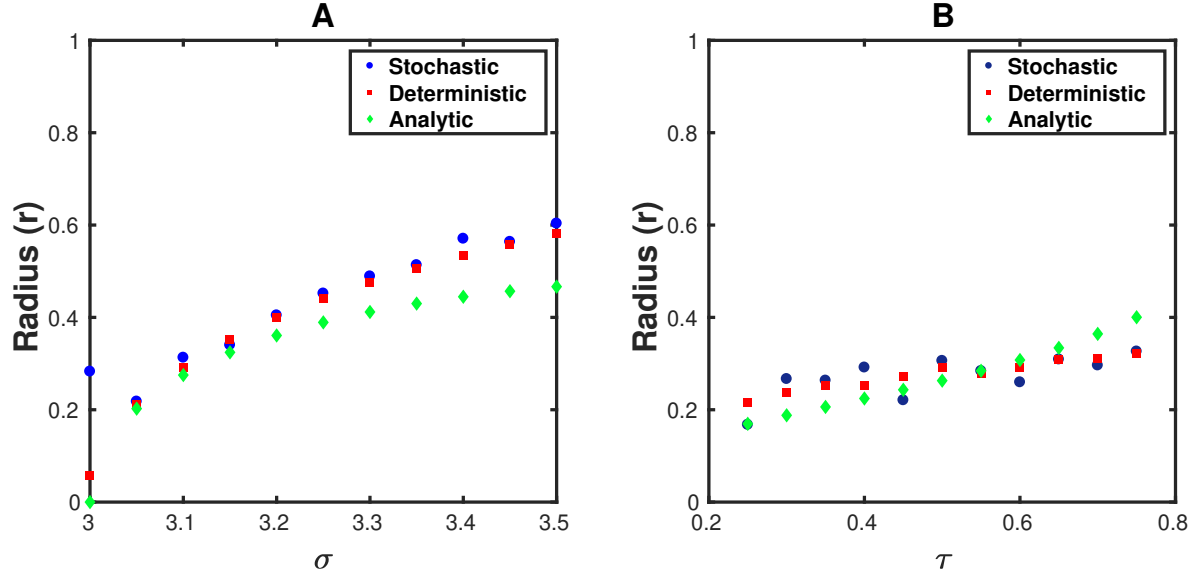


FIG. 4. Comparison of stochastic, deterministic, and analytical radius values versus different model parameters. Panel A shows the radius as a function of  $\sigma$  for  $\tau = 0.5$ . Panel B shows the radius as a function of  $\tau$  for  $\gamma = 0.06$ . In both panels  $a = 1$  and  $N = 25000$ .



## B. Angular Brownian Motion and The Noise Strength

In addition to producing amplitude fluctuations, demographic stochasticity also determines fluctuations in the phase of these oscillations. In this section we focus on the latter. In that context, it is natural to approximate the phase trajectory as an angular Brownian motion [18], with fixed frequency (corresponding to the one of eq. 9), and an angular diffusion term, with diffusion constant  $D$ . This ansatz is consistent with the results of figure 2, where the time evolution of the phase oscillates around a constant frequency. Therefore, the corresponding effective Langevin equation [18] for the angular position  $\theta$  can be written as follows:

$$\dot{\theta} = \omega + \sqrt{D}\xi(t) , \quad (10)$$

where  $D$  is the diffusion constant and  $\xi(t)$  is a white, delta correlated, Gaussian noise.

Eq. 10 predicts that the variance of  $\theta$  (calculated across independent realizations of the process starting from the same initial conditions) grows at  $Dt$ . Figure 5 shows that, in agreement with the Geometric Brownian Motion ansatz, the variance of the phase increase linearly with time.

The diffusion constant  $D$  plays the role of an effective parameter, capturing the effect of stochasticity on the limit cycle trajectories. Our goal is to determine, in the linear noise approximation, the dependency of this effective diffusivity  $D$  on the parameters of the RMA model ( $a$ ,  $\sigma$ , and  $\tau$ ) as well as on the population size  $N$ .

Given the demographic nature of the noise, we expect fluctuations to become less and less important with increasing  $N$ . Figure 5 shows that, as expected,  $D$  has a reversed relationship with the system size  $N$ .

## C. Analytic Approximation for the Noise Strength

In order to study the perturbations during evolution of the system around the limit cycle, we write the Fokker-Planck equation [18] of the stochastic RMA model by expanding the

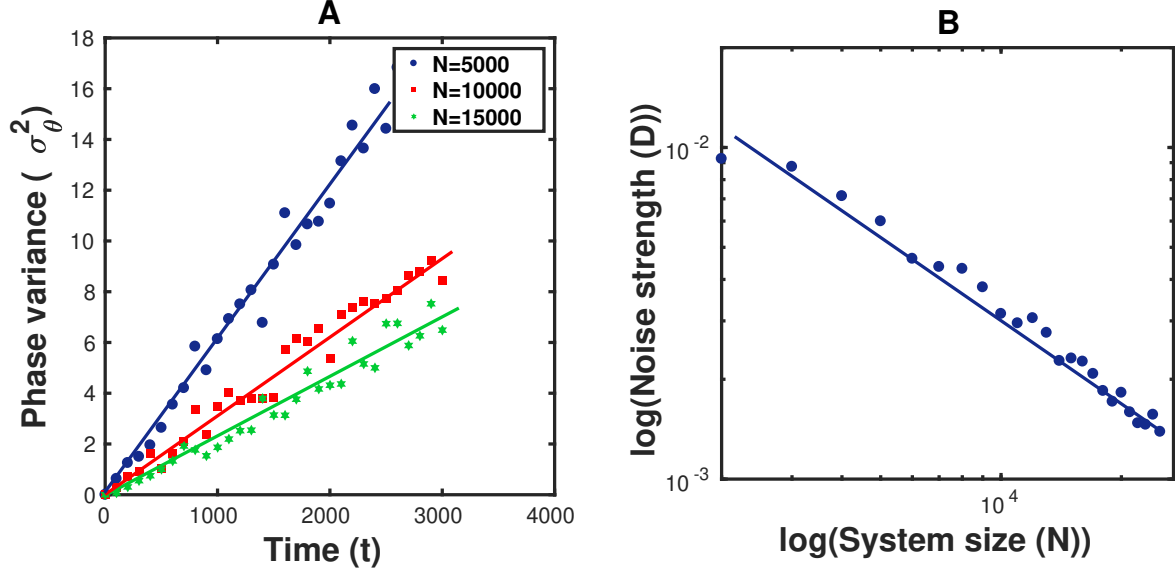


FIG. 5. Quantifying the noise strength along the limit cycle. (A) Phase variance over time for different values of system size. (B) the noise strength versus  $N$ . Parameters in these figures are  $\tau = 0.5$ ,  $a = 1$  and  $\sigma = 3.05$  and the variance is calculated over 500 realizations of the system.

master equation for large values of  $N$ . We obtain the following equation:

$$\begin{aligned}
 \partial_t P(x, y) = & -\frac{\partial}{\partial x} F_x P(x, y) - \frac{\partial}{\partial y} F_y P(x, y) \\
 & + \frac{1}{2N} \frac{\partial^2}{\partial x^2} B_{xx} P(x, y) + \frac{1}{2N} \frac{\partial^2}{\partial y^2} B_{yy} P(x, y) \\
 & + \frac{1}{2N} \frac{\partial^2}{\partial x \partial y} B_{xy} P(x, y) + \frac{1}{2N} \frac{\partial^2}{\partial y \partial x} B_{yx} P(x, y),
 \end{aligned} \tag{11}$$

where  $P(x, y)$ , is the probability to find the system with abundances  $(x, y) = (R/N, F/N)$  at time  $t$  and:

$$\begin{aligned}
 F_x &= ax - \frac{x^2}{2} - \frac{\sigma xy}{1 + \sigma \tau x}, \\
 F_y &= \frac{\sigma xy}{1 + \sigma \tau x} - y, \\
 B_{xx} &= \frac{1}{N} \left( ax + \frac{x^2}{2} + \frac{\sigma xy}{1 + \sigma \tau x} \right), \\
 B_{yy} &= \frac{1}{N} \left( \frac{\sigma xy}{1 + \sigma \tau x} + y \right), \\
 B_{xy} &= B_{yx} = -\frac{1}{N} \left( \frac{\sigma xy}{1 + \sigma \tau x} \right).
 \end{aligned} \tag{12}$$

In the limit of weak noise, the Fokker-Planck equation can be expanded around the deterministic solution, scaled by the square root of the noise amplitude ( $\mathbf{v} = \frac{1}{\sqrt{N}}(\mathbf{x} - \mathbf{x}_{\text{det}})$ ).

This is called Van Kampen expansion [18, 19] and it has been previously applied in the context of ecological models with demographic stochasticity [20]. Under the Van Kampen expansion, by omitting terms of higher order in  $(1/N)^{-1/2}$ , the Fokker-Planck equation can be transformed to the following equation:

$$\begin{aligned} \partial_t P(\mathbf{v}, t) = & - \sum_{i,j} A_{ij}(t) \frac{\partial}{\partial v_i} v_i P(\mathbf{v}, t) \\ & + \frac{1}{2} \sum_{i,j} \tilde{B}_{ij} \frac{\partial^2}{\partial v_i \partial v_j} P(\mathbf{v}, t), \end{aligned} \quad (13)$$

where

$$\begin{aligned} A_{ij} &= \frac{\partial F_i}{\partial v_j} \Big|_{\mathbf{x}_{\text{det}}(\mathbf{t})}, \\ \tilde{B}_{ij} &= B_{ij} \Big|_{\mathbf{x}_{\text{det}}(\mathbf{t})}. \end{aligned} \quad (14)$$

Since we approximated the shape of the limit cycle with an ellipse, we can write the deterministic solution in the following form:

$$\mathbf{x}_{\text{det}} = \mathbf{x}_f + \begin{bmatrix} r(t) \cos \theta(t) \\ \epsilon r(t) \sin \theta(t) \end{bmatrix}. \quad (15)$$

To investigate the stochastic RMA system, we decompose the noise term into the normal  $\xi_n$  and tangent  $\xi_l$  direction along the limit cycle, corresponding respectively to amplitude and phase fluctuations. The two components  $\xi_n$  and  $\xi_l$  can be obtained using:

$$\mathbf{x} = \mathbf{x}_{\text{det}} + \left( r^*(t) + \frac{\xi_n}{\sqrt{N}} \right) \begin{bmatrix} \cos(\omega t + \frac{\xi_l}{\sqrt{N}}) \\ \epsilon \sin(\omega t + \frac{\xi_l}{\sqrt{N}}) \end{bmatrix}, \quad (16)$$

in this equations  $r^* = \langle r \rangle$  and  $\omega = \epsilon$  according to the eq. 9. By expanding the noise terms for large  $N$  we find that:

$$\mathbf{x}_{\text{det}} = \mathbf{x}_f + \begin{bmatrix} r^*(t) \cos(\omega t) \\ \epsilon r^*(t) \sin(\omega t) \end{bmatrix} + \left( \frac{1}{\sqrt{N}} \right) \begin{bmatrix} \xi_x \\ \xi_y \end{bmatrix}, \quad (17)$$

where

$$\begin{aligned} \xi_x &= \xi_n \cos(\omega t) - \xi_l r^*(t) \sin(\omega t), \\ \xi_y &= \xi_n \epsilon \sin(\omega t) - \xi_l \epsilon r^*(t) \cos(\omega t). \end{aligned} \quad (18)$$

The Langevin equation corresponding to the  $\xi_x$  and  $\xi_y$  are written as:

$$\begin{aligned}\dot{\xi}_x &= \sum_i A_{x,i} + \eta_x, \\ \dot{\xi}_y &= \sum_i A_{y,i} + \eta_y,\end{aligned}\tag{19}$$

where  $\eta$  is related to the noise terms of Fokker-Planck equations as following:

$$\begin{aligned}\langle \eta_x^2 \rangle &= B_{xx}, \\ \langle \eta_y^2 \rangle &= B_{yy}, \\ \langle \eta_x \eta_y \rangle &= B_{xy}.\end{aligned}\tag{20}$$

The value of  $\langle \dot{\xi}_l^2 \rangle$  can be found by straight forward calculations from equations 18 and 19 as follows

$$\begin{aligned}\langle \dot{\xi}_l^2 \rangle &= \langle \dot{\xi}_l^2 \rangle_{det} + Dt, \\ D &= \frac{1}{2r^2\epsilon^2N} \left[ \epsilon^2 \left( ax + \frac{x^2}{2} + \frac{xy\sigma}{1+x\tau\sigma} \right) + y + \frac{xy\sigma}{1+x\tau\sigma} \right].\end{aligned}\tag{21}$$

Where the averaging is over different realizations and one period of time. Figure 5 shows the noise strength inferred from stochastic simulations, decreases as  $1/\sqrt{N}$  as predicted by our analytical calculation. Figure 6 shows the dependency of the effective diffusion constant  $D$  on the parameters  $\sigma$  and  $\tau$ . In the regime where our approximation is expected to work, i.e., when  $\sigma$  is close to the  $\sigma^*$  (i.e.,  $\gamma \rightarrow 0$ ) the results of analytical approximation matches well the numerical simulations.

#### IV. DISCUSSION

Oscillatory behavior in the populations has been widely reported in natural ecosystems and laboratory-scale experiments. Mathematical modeling of the interaction between predator and prey populations leads to the nonlinear ordinary differential equations that the time-dependent solutions of them are associated with limit cycle oscillations. Demographic stochasticity, due to unpredictability of the timing of birth, death, and interaction events, is often neglected and can remarkably alter the dynamics of a system.

In this paper, we have quantified the strength of the perturbations, due to the demographic effects of interacting species, in the limit cycle of the Roseznweig-MacArthur model.

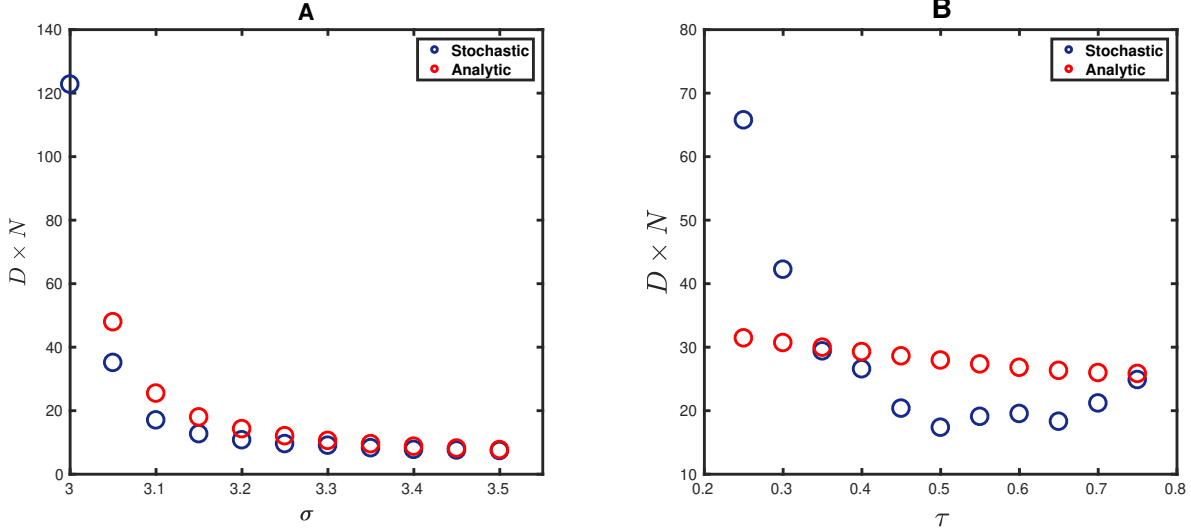


FIG. 6. Comparison of the stochastic and analytical noise strength for different parameters. Parameters are  $\gamma = 0.03$ ,  $a = 1$ ,  $\tau = 0.5$  and  $N = 25000$ .

We showed that, in the vicinity of the bifurcation point, the limit cycle shape is well approximated by an ellipse. In this limit, we obtained analytically the mean frequency and mean radius of the limit cycle as functions of the model parameters.

We then focus on the effect of stochasticity on the fluctuations along the limit cycle, that we effectively model as an angular Brownian motion. By expanding the master equation of the population densities through the Van Kampen system size method, we found demographic noise strength analytically, which has an inverse relationship with the system size. Finally, we compared our analytical results with the results found using simulation of the stochastic Rosenzweig-MacArthur model by Gillespie algorithm. A close agreement is observed between analytical results and the results found from the simulations.

Our work shows how the effect of demographic stochasticity on the frequency and phase of oscillation can be analytically captured even for non-linear model. Our calculation can be potentially extended to consider different sources of stochasticity (e.g. environmental) or to analyses oscillations in spatially extended systems.

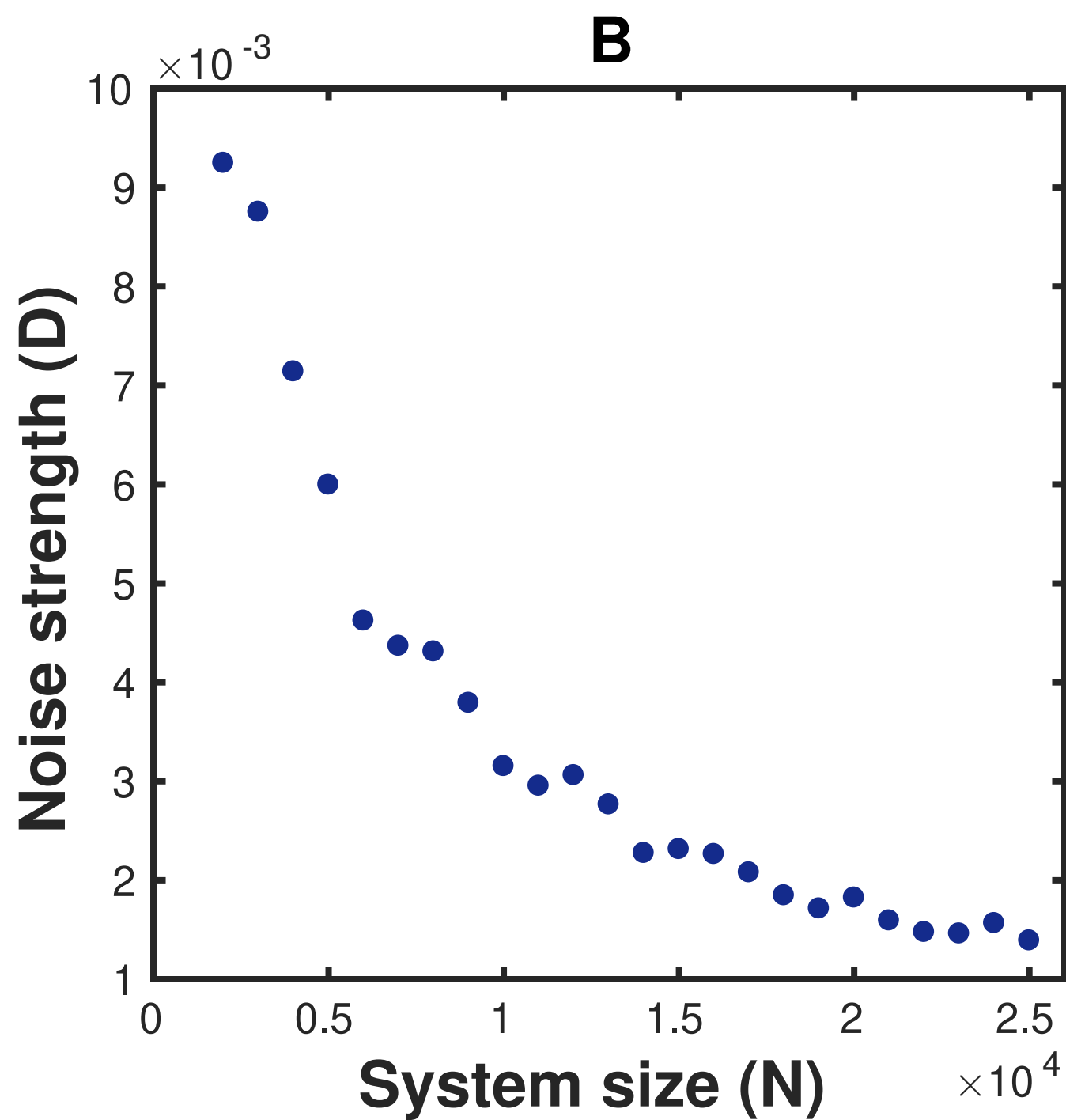
## ACKNOWLEDGMENTS

SG acknowledges the ICTP STEP program for the support for her visits to The Abdus Salam ICTP.

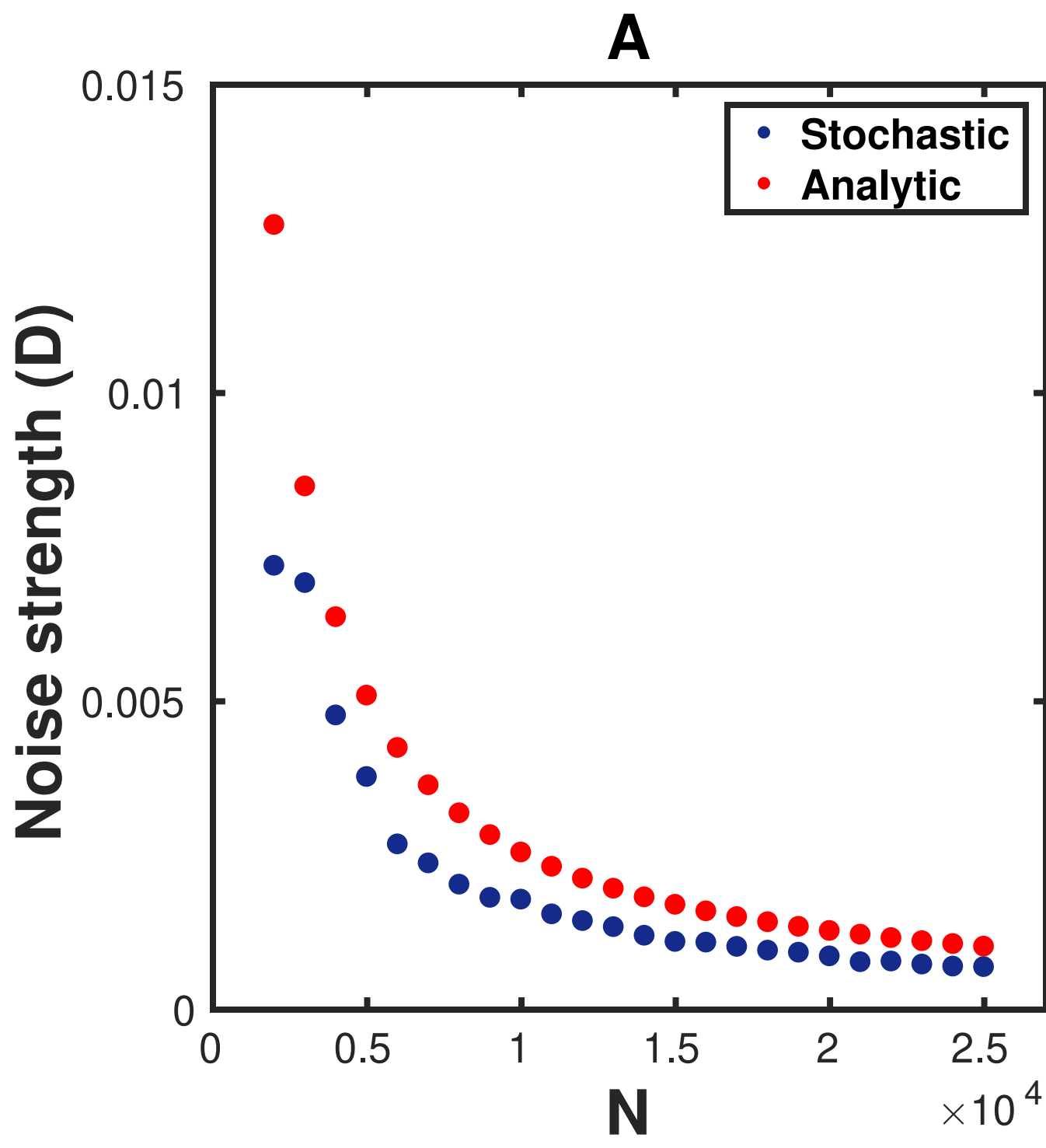
---

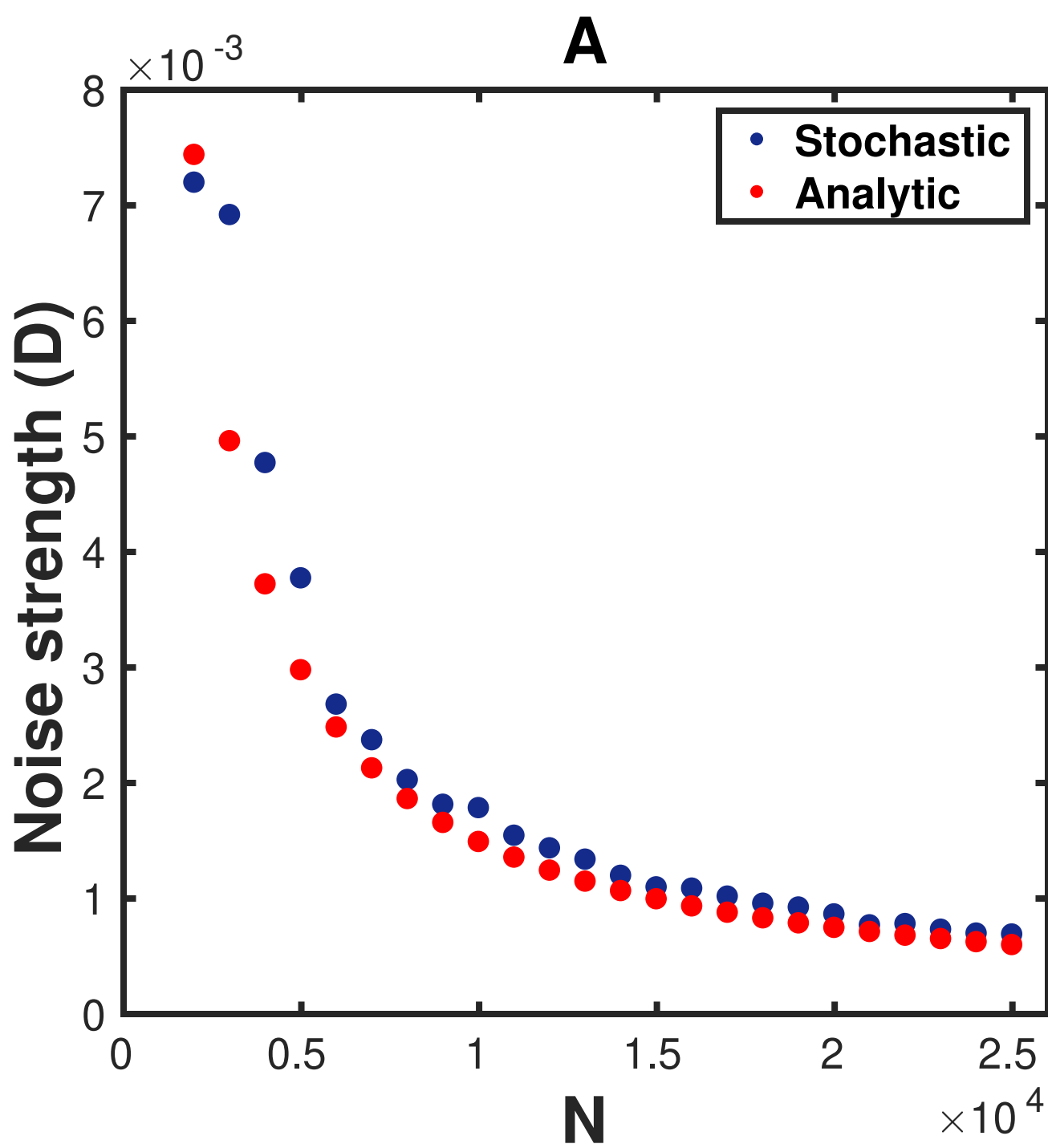
- [1] A. J. Lotka, Analytical note on certain rhythmic relations in organic systems, Proceedings of the National Academy of Sciences **6**, 410 (1920).
- [2] V. Volterra, *Variazioni e fluttuazioni del numero d'individui in specie animali conviventi*, Vol. 2 (Società anonima tipografica" Leonardo da Vinci", 1927).
- [3] M. L. Rosenzweig and R. H. MacArthur, Graphical representation and stability conditions of predator-prey interactions, The American Naturalist **97**, 209 (1963).
- [4] C. S. Holling, The components of predation as revealed by a study of small-mammal predation of the european pine sawfly<sup>1</sup>, The canadian entomologist **91**, 293 (1959).
- [5] M. E. Gilpin, Do hares eat lynx?, The American Naturalist **107**, 727 (1973).
- [6] C. Elton and M. Nicholson, The ten-year cycle in numbers of the lynx in canada, The Journal of Animal Ecology , 215 (1942).
- [7] L. Butler, The nature of cycles in populations of canadian mammals, Canadian Journal of Zoology **31**, 242 (1953).
- [8] E. Korpimäki, K. Norrdahl, O. Huitu, and T. Klemola, Predator-induced synchrony in population oscillations of coexisting small mammal species, Proceedings of the Royal Society B: Biological Sciences **272**, 193 (2005).
- [9] K. Higgins, A. Hastings, J. N. Sarvela, and L. W. Botsford, Stochastic dynamics and deterministic skeletons: population behavior of dungeness crab, Science **276**, 1431 (1997).
- [10] N. Kamata and A. Liebhold, Are population cycles and spatial synchrony a universal characteristic of forest insect populations?, Population Ecology **42** (2000).
- [11] R. M. May, Stability in randomly fluctuating versus deterministic environments, The American Naturalist **107**, 621 (1973).
- [12] B. A. Melbourne and A. Hastings, Extinction risk depends strongly on factors contributing to stochasticity, Nature **454**, 100 (2008).
- [13] S. Petrovskii, A. Morozov, H. Malchow, and M. Sieber, Noise can prevent onset of chaos in

- spatiotemporal population dynamics, *The European Physical Journal B* **78**, 253 (2010).
- [14] D. C. Reuman, R. F. Costantino, R. A. Desharnais, and J. E. Cohen, Colour of environmental noise affects the nonlinear dynamics of cycling, stage-structured populations, *Ecology Letters* **11**, 820 (2008).
  - [15] A. J. Black and A. J. McKane, Stochastic amplification in an epidemic model with seasonal forcing, *Journal of Theoretical Biology* **267**, 85 (2010).
  - [16] K.-S. Cheng, Uniqueness of a limit cycle for a predator-prey system, *SIAM Journal on Mathematical Analysis* **12**, 541 (1981), <https://doi.org/10.1137/0512047>.
  - [17] N. R. Smith and B. Meerson, Extinction of oscillating populations, *Physical Review E* **93**, 032109 (2016).
  - [18] C. W. Gardiner *et al.*, *Handbook of stochastic methods*, Vol. 3 (springer Berlin, 1985).
  - [19] N. G. Van Kampen, *Stochastic processes in physics and chemistry*, Vol. 1 (Elsevier, 1992).
  - [20] A. J. Black and A. J. McKane, Stochastic formulation of ecological models and their applications, *Trends in Ecology & Evolution* **27**, 337 (2012).

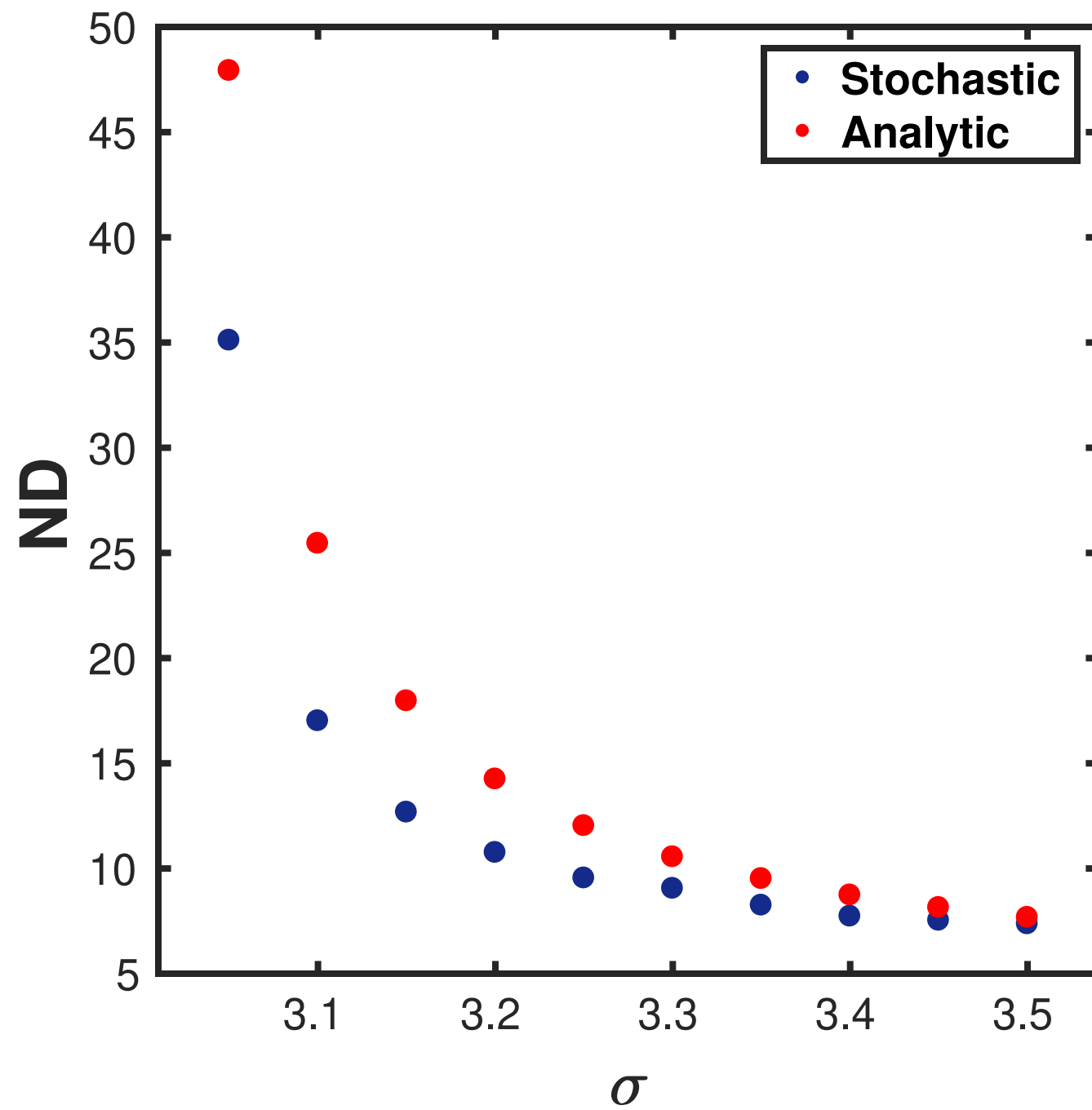


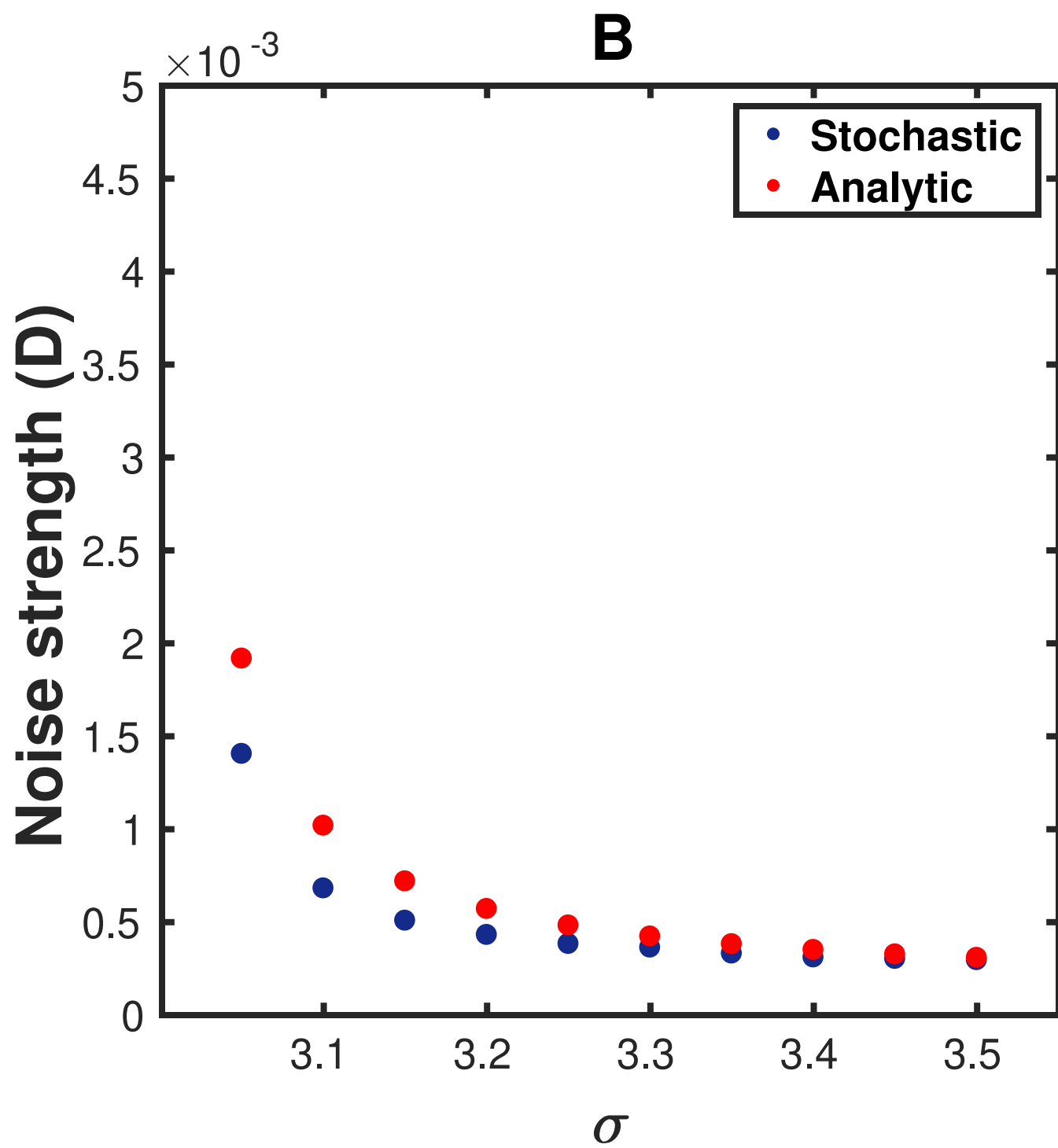


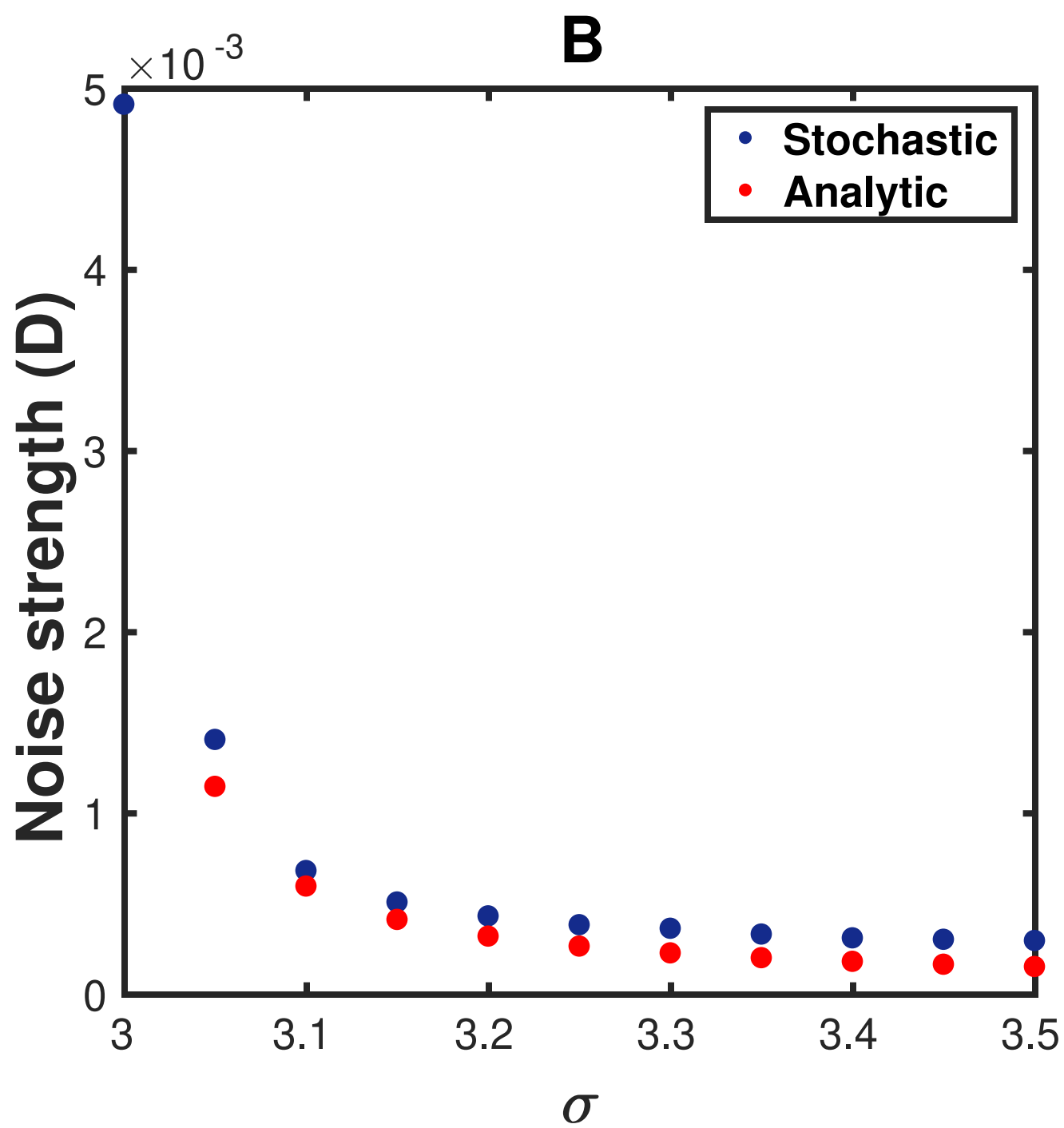




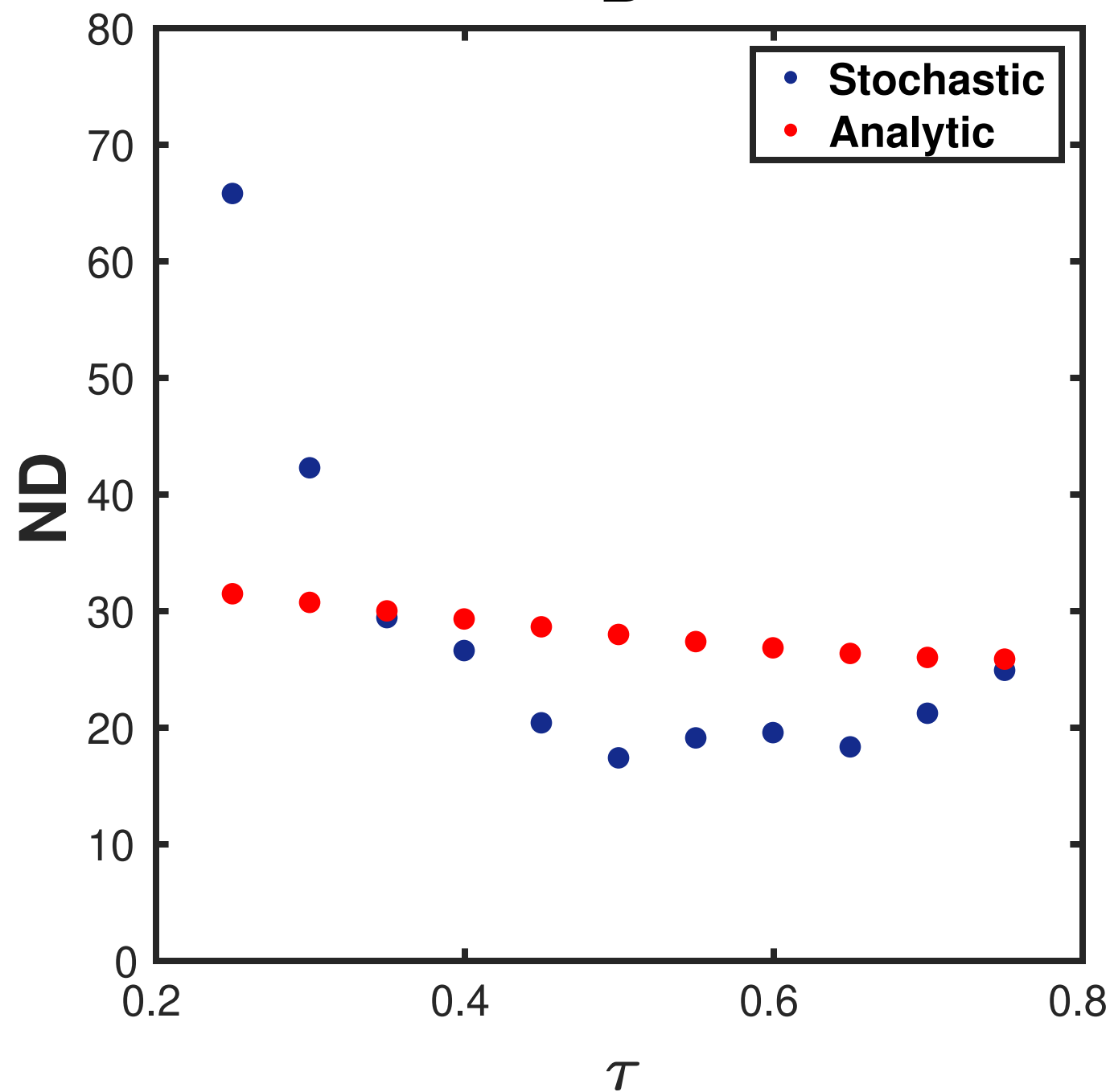
**A**

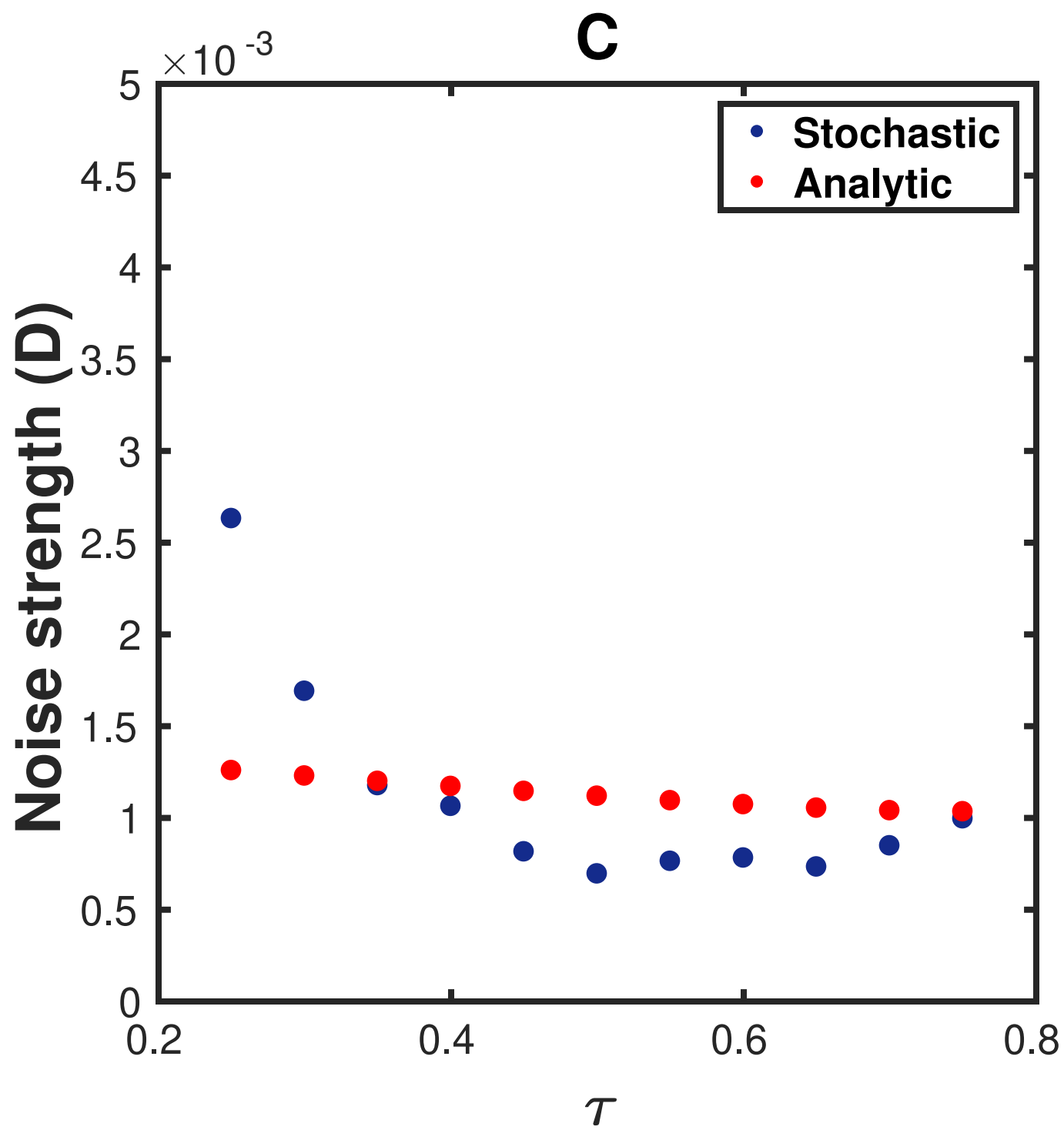


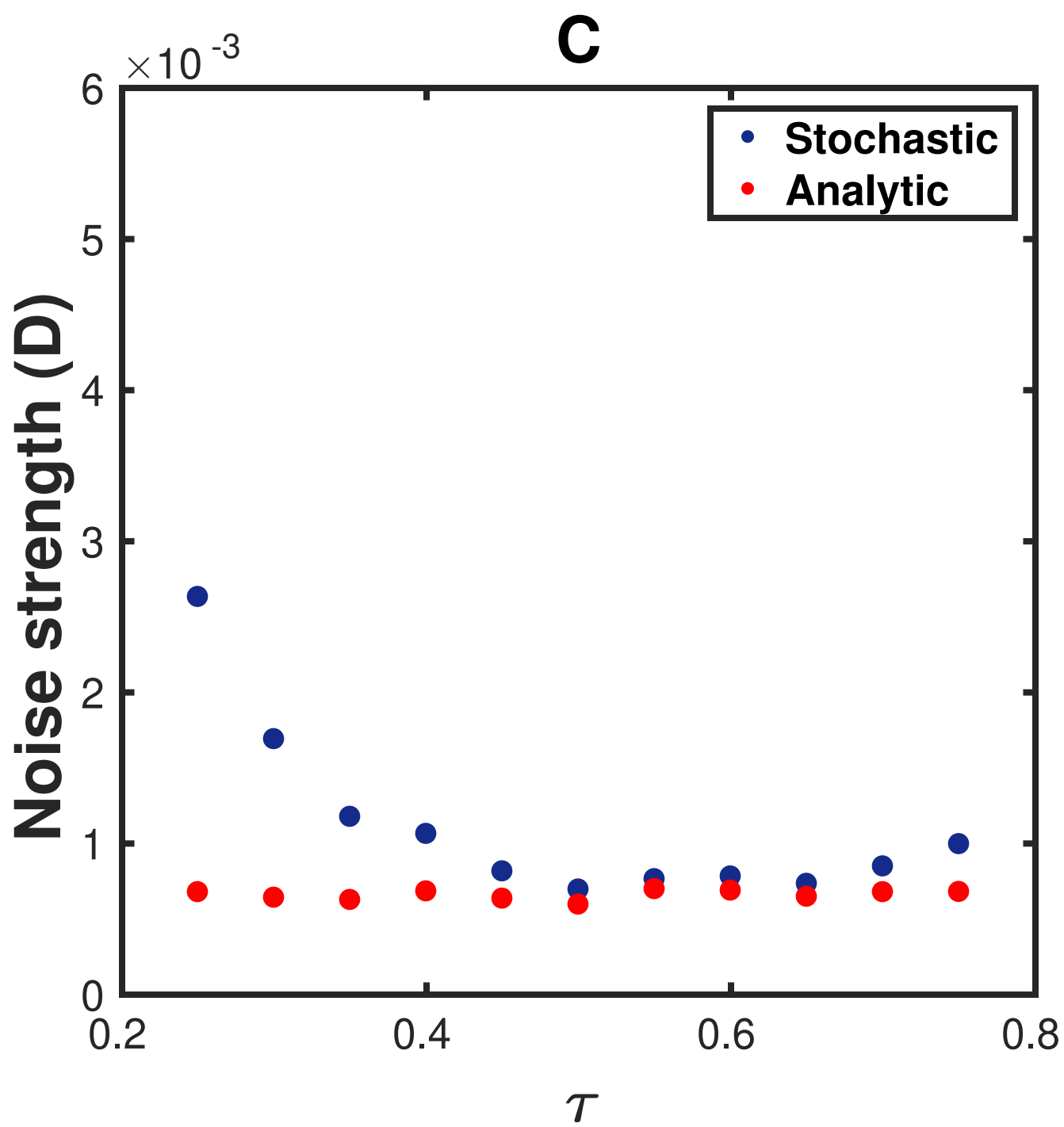




**B**

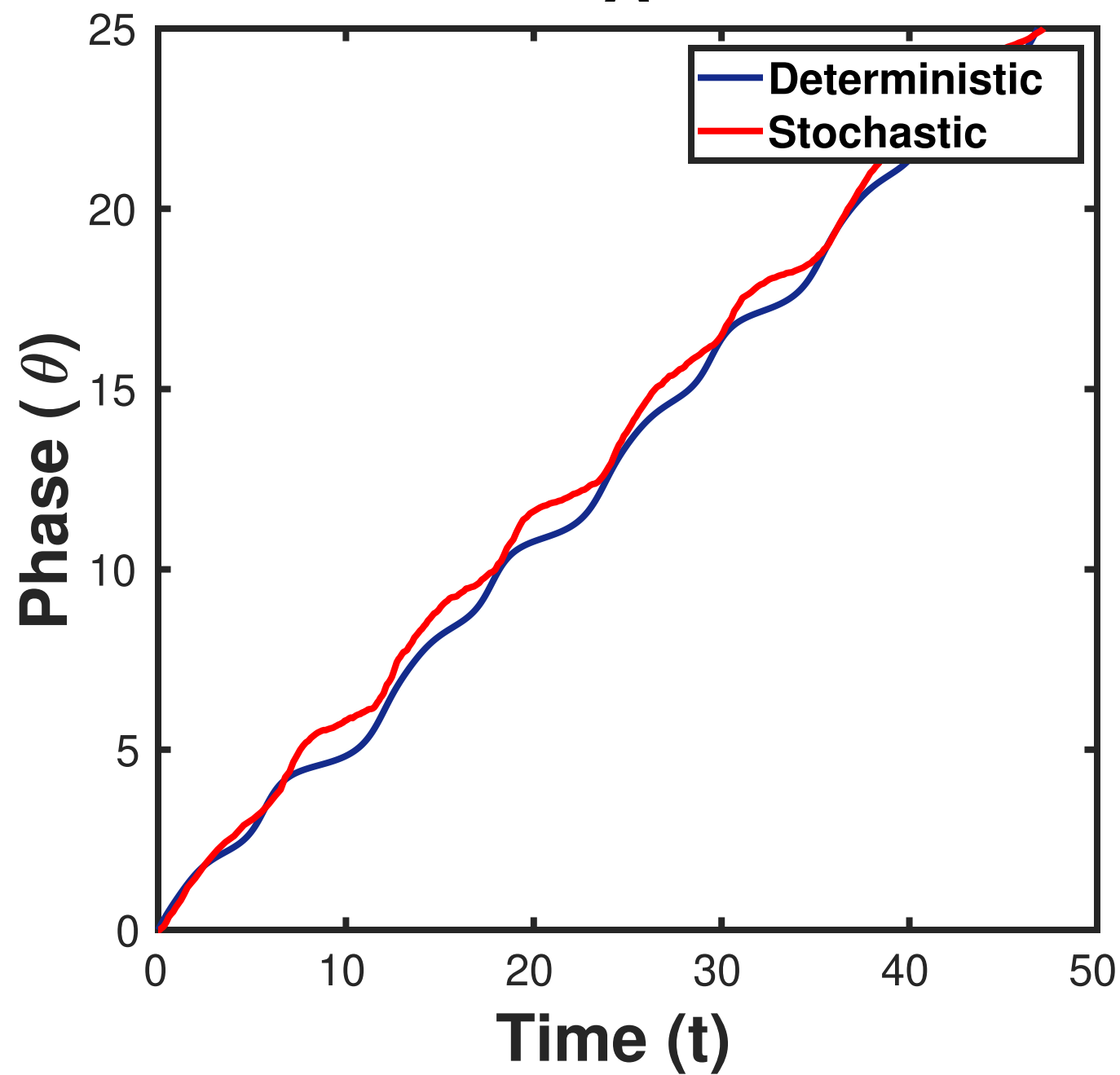








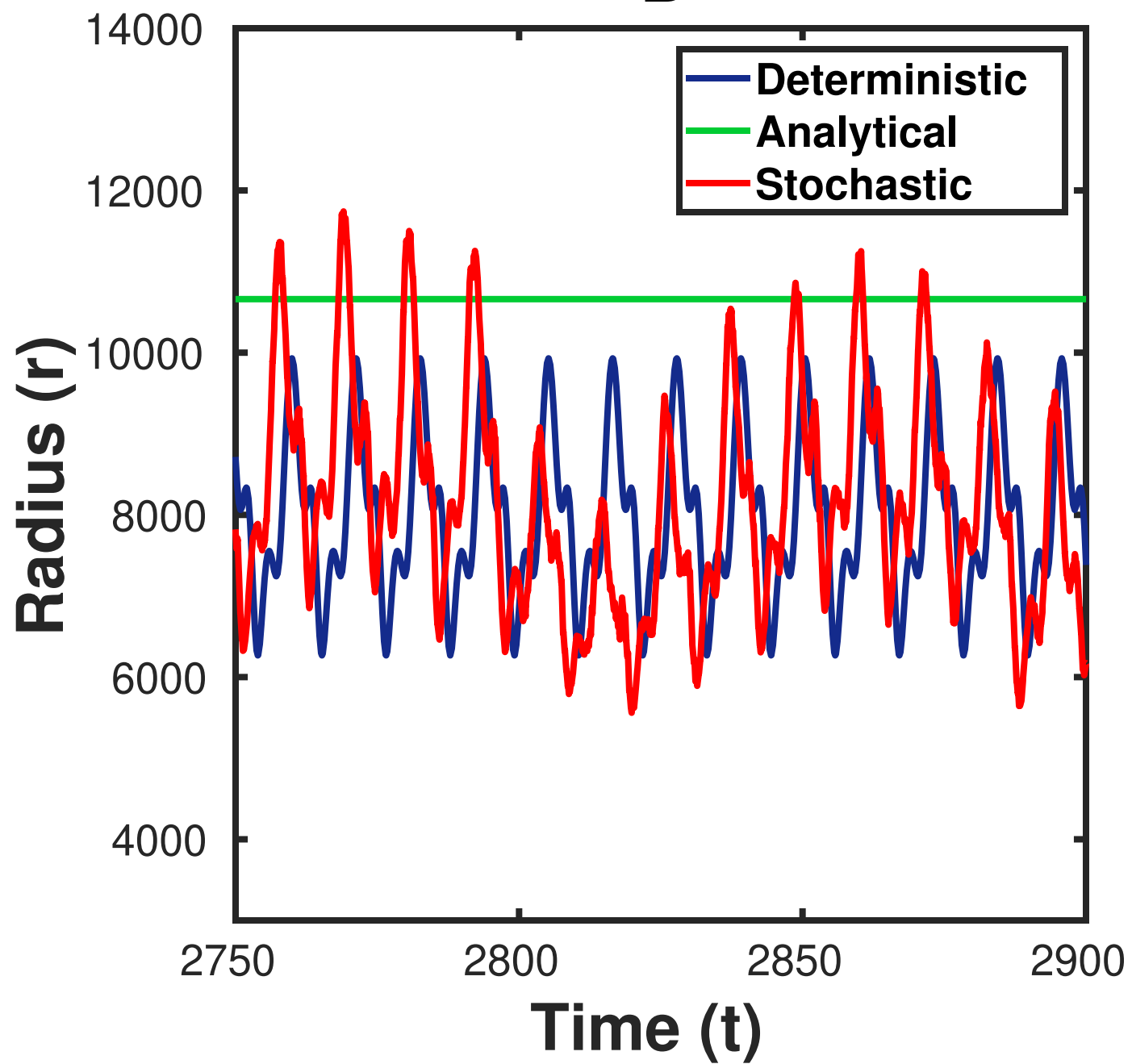
**A**



This figure "THREE-A.jpg" is available in "jpg" format from:

<http://arxiv.org/ps/2310.20575v2>

**B**



This figure "THREE-B.jpg" is available in "jpg" format from:

<http://arxiv.org/ps/2310.20575v2>

This figure "TWO0.jpg" is available in "jpg" format from:

<http://arxiv.org/ps/2310.20575v2>